

Intersubband absorption in AlN/GaN/AlGaN coupled quantum wells

Kristina Driscoll, Anirban Bhattacharyya, Theodore D. Moustakas, and Roberto Paiella^{a)}
 Department of Electrical and Computer Engineering and Photonics Center, Boston University, 8
 Saint Mary's Street, Boston, Massachusetts 02215, USA

Lin Zhou and David J. Smith

Department of Physics and School of Materials, Arizona State University, Tempe, Arizona 85287, USA

(Received 28 July 2007; accepted 13 September 2007; published online 1 October 2007)

AlN/GaN/AlGaN coupled quantum wells grown by molecular beam epitaxy have been developed and characterized via intersubband absorption spectroscopy. In these structures, an AlGaN layer of sufficiently low Al content is used to achieve strong interwell coupling without the need for ultrathin inner barriers. At the same time, AlN is used in the outer barriers to provide the large quantum confinement required for near-infrared intersubband transitions. The composition of the inner barriers also provides a continuously tunable parameter to control the coupling strength. Double intersubband absorption peaks are measured in each sample, at photon energies in good agreement with theoretical expectations. © 2007 American Institute of Physics. [DOI: 10.1063/1.2794013]

Semiconductor quantum wells (QWs) based on group-III nitride compounds can provide extremely large conduction-band offsets and therefore accommodate electronic intersubband (ISB) transitions at record short wavelengths. In particular, extensive experimental work in the past several years has widely established that near-infrared ISB transitions at fiber-optic communication wavelengths can be obtained in relatively narrow GaN/AlN QWs.¹⁻⁵ Moreover, the strong electron-phonon interaction in these materials due to their highly polar nature yields particularly fast (subpicosecond) ISB relaxation lifetimes. These properties open up new opportunities for ISB device development, particularly in the area of all-optical switching for ultrafast fiber-optic communications.^{6,7} Other infrared technologies also being explored include photodetectors,⁸ electro-optic modulators,⁹ and, with the recent demonstration of optically pumped luminescence, light emitters.¹⁰

So far ISB transitions in III-nitride materials have been primarily studied using isolated GaN/Al(GaN) QWs. However, the development of coupled QWs (CQWs) is also highly desirable to extend the functionality and design flexibility of III-nitride based ISB devices. For example, CQWs can be used to engineer the ISB nonlinear optical properties, e.g., for resonance enhanced frequency conversion¹¹ or to reduce the saturation power of all-optical switching devices.¹² Similarly, CQWs can be used to implement three- (or four-) level systems with the required oscillator strengths and nonradiative lifetimes necessary for the development of optically pumped ISB lasers¹³ and ultimately, quantum cascade lasers. Yet, the study of III-nitride CQWs has so far been limited to only a few experimental demonstrations involving AlGaN/GaN (Ref. 14) or AlN/GaN systems.^{15,16}

From a design perspective, the development of strongly coupled III-nitride QWs is complicated by two basic properties of these heterostructures, namely, their heavy electronic effective masses m^* and large conduction-band offsets (which on the other hand enable the ISB transition wavelength to be extended to the near infrared as just discussed). As a result, in these QWs, the penetration depths of the

bound-state wavefunctions into the potential barriers (given by $l = \hbar / \sqrt{2m^*(E_B - E)}$, where E_B is the barrier energy and E the bound-state energy) are typically very small (a few angstroms). Thus, similarly small barrier thicknesses are in general required for strong interwell coupling. The use of such ultrathin barriers is, however, undesirable since it results in bound-state energies and wavefunctions that are exceedingly sensitive to even monolayer-scale thickness fluctuations. Additionally, it leaves very little design flexibility in fine tuning the degree of interwell coupling.

In this letter, we introduce an alternative approach to the development of III-nitride CQWs, where an AlGaN alloy of sufficiently small Al content (i.e., sufficiently low conduction-band edge) is used in the inner barrier to achieve strong coupling. At the same time, AlN is used in the outer barriers to provide the large quantum confinement required for ISB transitions at near-infrared wavelengths. These structures were designed using the Schrödinger-Poisson solver described below; an example is shown in Fig. 1, where we plot the calculated conduction-band lineup and bound-state envelope functions of an AlN/GaN/Al_{0.39}Ga_{0.61}N CQW system. Even though a relatively thick inner barrier of 5 monolayers (ML) is used in this design, the ground states |1⟩ and

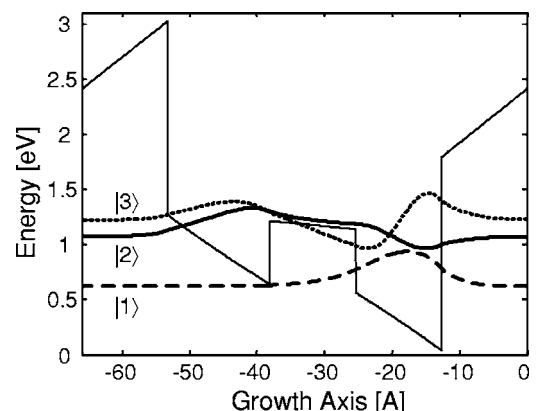


FIG. 1. Calculated conduction-band lineup and envelope functions of the three lowest bound states (referenced to their respective energy levels) of an AlN/GaN/AlGaN CQW structure, corresponding to sample A of Table I.

^{a)}Electronic mail: rpaiella@bu.edu

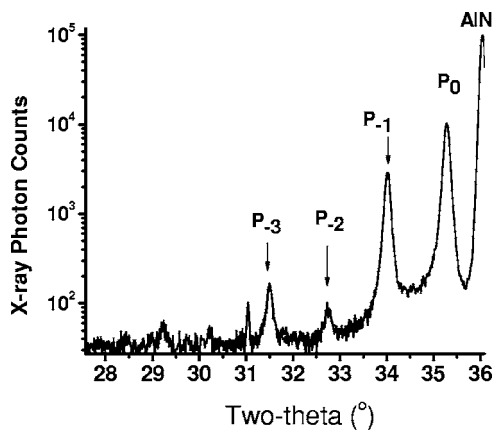


FIG. 2. On-axis θ - 2θ x-ray diffraction scan of sample C.

$|2\rangle$ of the two wells are optically coupled to each other by a sizeable electric dipole moment of about 3.6 \AA . By comparison, obtaining similar $|1\rangle$ - $|2\rangle$ and $|1\rangle$ - $|3\rangle$ transition energies and dipole moments with AlN/GaN/AlN CQWs would require ultrathin AlN inner barriers of nearly 1 ML. Moreover, the Al content x of the inner barrier provides a continuously tunable design parameter to control the QW coupling strength. In particular, in the limit $x \rightarrow 0$, the CQW potential profile approaches that of an isolated QW, where only a single ISB absorption peak, associated with the $|1\rangle$ - $|2\rangle$ transition, is typically resolved.¹⁷ Conversely, as x is increased, the degree of interwell coupling is reduced, and the strength of the “intrawell” transition $|1\rangle$ - $|3\rangle$ is increased relative to that of the interwell transition $|1\rangle$ - $|2\rangle$.

Three AlN/GaN/AlGaN CQW structures of different AlGaN compositions (labeled A, B, and C in the following) were grown for this study, using a Varian Gen-II plasma-assisted molecular beam epitaxy reactor. After nitridation of the c -plane sapphire substrates, an AlN buffer layer ($\sim 0.4 \mu\text{m}$ thick in samples A and B, $\sim 1.5\text{-}\mu\text{m}$ thick in sample C) was first deposited followed by 30 CQW periods and by an $\sim 0.2\text{-}\mu\text{m}$ -thick AlN cap. All layers were formed under group-III-rich conditions to promote two-dimensional growth. Since Al atoms are not readily desorbed from the surface at the growth temperature of $770 \text{ }^\circ\text{C}$, growth interruption under nitrogen flux was performed after deposition of each Al(Ga)N layer to consume excess Al accumulated on the surface. While this procedure allows for improved thickness control, it may also result in enhanced surface roughness depending on the duration of the growth interruption. Thus, a small flux of In was also used during growth of the Al(Ga)N layers because of the beneficial role played by In as a surfactant.¹⁸ The In flux was chosen to guarantee sufficient surface coverage without incorporation. In order to populate the lowest electronic bound state in each CQW, the wider wells were doped n type with Si to the level of a few 10^{19} cm^{-3} .

The structural properties of the three samples were characterized by high-resolution x-ray diffraction (HRXRD), cross-sectional transmission electron microscopy (XTEM), and Rutherford backscattering. HRXRD data are shown in Fig. 2 where we plot an on-axis θ - 2θ scan for sample C: several superlattice peaks are clearly resolved, indicating excellent periodicity of the overall CQW structure. The smaller amplitude of the second satellite peak P_{-2} relative to the third one P_{-3} is an interference effect, which has also been

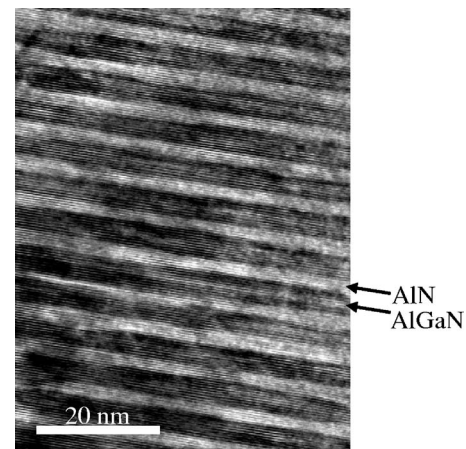


FIG. 3. Cross-section electron micrograph of sample C. The darker and lighter areas correspond to GaN and AlN, respectively. The AlGaN barriers appear as gray regions between the coupled GaN wells.

previously observed in GaN/AlGaN superlattices.¹⁹ From these HRXRD data and our calibrated growth rates, the individual layer thicknesses were estimated. An XTEM image of the same sample is shown in Fig. 3, where very well defined AlN/GaN interfaces are observed. The inner AlGaN barriers are also visible, although their clarity is limited by the image contrast. Finally, the coupling-barrier Al content for each sample was computed from the individual layer thicknesses and the average Al concentration, as measured by Rutherford backscattering. The resulting parameters are listed in Table I, where each thickness has been rounded off to an integral number of monolayers (with $1 \text{ ML} \approx 2.5 \text{ \AA}$). In each case, period-to-period and in-plane thickness variations by at least 1 ML should be considered, so that the three samples are in fact very similar to one another with regard to the well and barrier widths. On the other hand, they differ substantially in the Al concentration of the coupling barrier, which increases from 39% in sample A to 48% in B to 53% in C.

The ISB absorbance spectra of the three CQW structures were measured at room temperature with a Fourier transform infrared (FTIR) spectrometer and a cooled HgCdTe detector. To achieve a multipass waveguide geometry, the substrate of each sample was mirror polished and two opposite facets were lapped at 45° . Light from the FTIR internal source was then coupled in and out at normal incidence through these facets. In order to exclude effects due to the substrate, the infrared transmission spectra of p - and s -polarized light were normalized with respect to those through identically polished bare sapphire samples.

TABLE I. Estimated layer thicknesses (starting from the AlN outer barrier) and coupling-barrier Al content of the three samples studied in this work, and corresponding experimental and theoretical energies of the $|1\rangle$ - $|2\rangle$ and $|1\rangle$ - $|3\rangle$ ISB transitions.

Sample	Thicknesses (MLs)	Inner-barrier Al content (%)	Measured transition energies (meV)	Computed transition energies (meV)
A	10/6/5/5	39	429/611	454/602
B	9/5/5/5	48	457/631	461/619
C	11/7/5/5	53	465/626	445/625

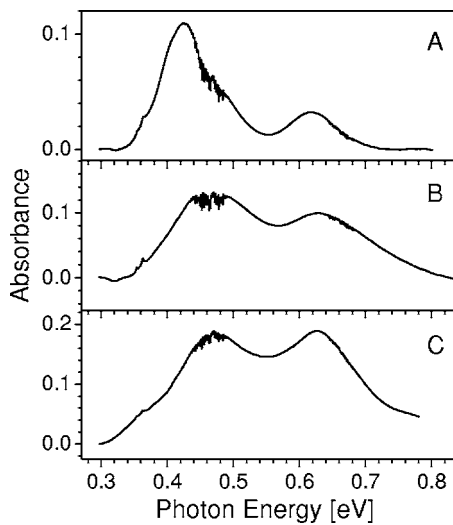


FIG. 4. Measured ISB absorbance spectra of samples A, B, and C.

The resulting ISB absorbance spectra are shown in Fig. 4. Two pronounced peaks are observed in each sample, at photon energies in good agreement with theoretical expectations for the $|1\rangle\text{-}|2\rangle$ and $|1\rangle\text{-}|3\rangle$ transition energies as discussed below. From these data and the computed dipole moments, we estimate an electron concentration in the range of $(1\text{--}3) \times 10^{12} \text{ cm}^{-2}$ for the three samples, consistent with the doping densities used. The spectral linewidths (full width at half maximum) of these features range between ~ 90 and 200 meV , which are comparable to the values measured in previous reports of III-nitride CQWs.^{14–16} These are reasonable linewidths for this class of materials, especially considering that ISB absorption in CQWs involves wavefunctions delocalized over up to four heterojunctions. Another important feature of Fig. 4 is the relative absorption strength of the interwell $|1\rangle\text{-}|2\rangle$ transition with respect to the intrawell $|1\rangle\text{-}|3\rangle$ transition, which is seen to decrease in going from sample A to B to C. This is consistent with the corresponding increase in Al content of the inner barrier, which results in a reduced degree of interwell coupling. These data thus illustrate the ability to tune the coupling strength provided by this design approach.

The structures developed in this work were modeled with a self-consistent Poisson and Schrödinger equation solver based on the effective-mass approximation. The characteristic built-in electric fields of GaN/Al(GaN) QWs due to their spontaneous and piezoelectric polarizations were included explicitly in these calculations following, e.g., Ref. 20, and using periodic boundary conditions (i.e., requiring that the intrinsic voltage drop across each CQW period is zero). The nonparabolicity of the conduction band was also taken into account using experimentally determined parameters,²¹ as required when dealing with excited states at energies well above the band edge. The AlN/GaN conduction-band offset was taken to be 1.75 eV ;¹⁵ all other relevant material parameters were selected from Ref. 22. Theoretical values for the $|1\rangle\text{-}|2\rangle$ and $|1\rangle\text{-}|3\rangle$ transition energies of samples A, B, and C computed with this model are listed in Table I (the full conduction-band lineup of sample A is also shown in Fig. 1). The overall agreement between theory and experiments is quite good, with all calculated energies within less than 6% of the corresponding measured

values. We emphasize that a certain degree of uncertainty exists in several parameters used in these calculations. However, the identification of the measured absorption peaks with the $|1\rangle\text{-}|2\rangle$ and $|1\rangle\text{-}|3\rangle$ transitions is unambiguous, and no reasonable set of parameter values can reproduce the measurement results based on any other set of transitions.

In conclusion, the results presented here show that high-quality III-nitride CQWs can be developed using properly designed AlN/GaN/AlGaIn heterostructures. With this approach, fine tuning of the interwell coupling strength is possible by varying the Al content of the inner barriers. These quantum structures will be useful for the future development of advanced ISB devices based on nitride semiconductors.

This work was supported by the National Science Foundation under Grant No. ECS-0622102 and by the Army Research Laboratory. We acknowledge the use of facilities in the John M. Cowley Center for High Resolution Electron Microscopy at Arizona State University.

- ¹C. Gmachl, H. M. Ng, S.-N. G. Chu, and A. Y. Cho, *Appl. Phys. Lett.* **77**, 3722 (2000).
- ²K. Kishino, A. Kikuchi, H. Kanazawa, and T. Tachibana, *Appl. Phys. Lett.* **81**, 1234 (2002).
- ³N. Iizuka, K. Kaneko, and N. Suzuki, *Appl. Phys. Lett.* **81**, 1803 (2002).
- ⁴M. Tchernycheva, L. Nevou, L. Doyennette, F. H. Julien, E. Warde, F. Guillot, E. Monroy, E. Bellet-Amalric, T. Remmele, and M. Albrecht, *Phys. Rev. B* **73**, 125347 (2006).
- ⁵I. Friel, K. Driscoll, E. Kulevica, M. Dutta, R. Paiella, and T. D. Moustakas, *J. Cryst. Growth* **278**, 387 (2005).
- ⁶N. Iizuka, K. Kaneko, and N. Suzuki, *IEEE J. Quantum Electron.* **42**, 765 (2006).
- ⁷Y. Li, A. Bhattacharyya, C. Thomidis, T. D. Moustakas, and R. Paiella, *Opt. Express* **15**, 5860 (2007).
- ⁸D. Hofstetter, S.-S. Schad, H. Wu, W. J. Schaff, and L. F. Eastman, *Appl. Phys. Lett.* **83**, 572 (2003).
- ⁹E. Baumann, F. R. Giorgetta, D. Hofstetter, S. Leconte, F. Guillot, E. Bellet-Amalric, and E. Monroy, *Appl. Phys. Lett.* **89**, 101121 (2006).
- ¹⁰L. Nevou, M. Tchernycheva, F. H. Julien, F. Guillot, and E. Monroy, *Appl. Phys. Lett.* **90**, 121106 (2007).
- ¹¹F. Capasso, C. Sirtori, and A. Y. Cho, *IEEE J. Quantum Electron.* **30**, 1313 (1994).
- ¹²Y. Li and R. Paiella, *Semicond. Sci. Technol.* **21**, 1105 (2006).
- ¹³O. Gauthier-Lafaye, P. Boucaud, F. H. Julien, S. Sauvage, S. Cabaret, J. M. Lourtioz, V. Thierry-Mieg, and R. Planel, *Appl. Phys. Lett.* **71**, 3619 (1997).
- ¹⁴C. Gmachl, H. M. Ng, and A. Y. Cho, *Appl. Phys. Lett.* **79**, 1590 (2001).
- ¹⁵M. Tchernycheva, L. Nevou, L. Doyennette, F. H. Julien, F. Guillot, E. Monroy, T. Remmele, and M. Albrecht, *Appl. Phys. Lett.* **88**, 153113 (2006).
- ¹⁶L. Nevou, N. Kheirodin, M. Tchernycheva, L. Meignien, P. Crozat, A. Lupu, E. Warde, F. H. Julien, G. Pozzovivo, S. Golka, G. Strasser, F. Guillot, E. Monroy, T. Remmele, and M. Albrecht, *Appl. Phys. Lett.* **90**, 223511 (2007).
- ¹⁷Strictly speaking, the $|1\rangle\text{-}|3\rangle$ ISB transitions have nonzero dipole moment even in isolated GaN/Al(GaN) QWs due to the lack of mirror symmetry produced by the built-in electric fields of these heterostructures. However, these transitions are typically too weak to be observed in transmission measurements.
- ¹⁸A. Bhattacharyya, I. Friel, S. Iyer, T. C. Chen, W. Li, J. Cabalu, Y. Fedyunin, K. F. Ludwig, T. D. Moustakas, H. P. Maruska, D. W. Hill, J. J. Gallagher, M. C. Chou, and B. Chai, *J. Cryst. Growth* **251**, 487 (2003).
- ¹⁹D. Korakakis, K. F. Ludwig, and T. D. Moustakas, *Appl. Phys. Lett.* **72**, 1004 (1998).
- ²⁰O. Ambacher, B. Foutz, J. Smart, J. R. Shealy, N. G. Weimann, K. Chu, M. Murphy, A. J. Sierakowski, W. J. Schaff, L. F. Eastman, R. Dimitrov, A. Mitchell, and M. Stutzmann, *J. Appl. Phys.* **87**, 334 (2000).
- ²¹S. Syed, J. B. Heroux, Y. J. Wang, M. J. Manfra, R. J. Molnar, and H. L. Stormer, *Appl. Phys. Lett.* **83**, 4553 (2003).
- ²²I. Vurgaftman and J. R. Meyer, *J. Appl. Phys.* **94**, 3675 (2003).